Low Energy Ion Scattering Investigations of *n*-Butanol−Ice System in the Temperature Range of 110−150 K

G. Naresh Kumar, Jobin Cyriac,† Soumabha Bag, and T. Pradeep*

DST Unit on Nanoscience, Department of Chemistry and Sophisticated Analytical Instrument Facility, Indian Institute of Technology Madras, Chennai, India 600 036

Received: March 5, 2009; Revised Manuscript Received: June 8, 2009

We have investigated the interaction of *n*-butanol (NBA) with thin layers of water ice prepared in ultra high vacuum in the temperature range of 110−150 K. From the mass spectra of the chemically sputtered species, created upon the collision of low energy (≥30 eV) Ar^+ ions, we study the process of diffusive mixing of NBA with water ice, at the molecular level. The results show that NBA undergoes diffusive mixing with H_2O. Even after depositing 1000 monolayers (MLs) of amorphous solid water (ASW) over NBA, both the species are observed on the surface. However, when NBA is deposited over ASW, no water is seen on the surface above 3−5 MLs of NBA. This could be interpreted as the absence of diffusive mixing in this system or surface segregation of NBA, in view of its lower surface energy just as in the case of liquid alcohols. An isomeric alcohol, namely, *tert*-butyl alcohol (TBA), also behaves similarly. Although the presence of NBA and TBA is detected, in the presence of ASW, they undergo selective ionization, giving specific peaks in the mass spectrum. D_2O behaves in a manner similar to that of H_2O. Preliminary experiments with other alcohols; namely, methanol, ethanol, and propanol were also done, and the results suggest that incomplete diffusion or surface segregation begins with propanol.

1. Introduction

Ice particles in pure form as well as mixed with several molecules and ions are spread all over the Earth's atmosphere. The study of ice surface becomes interesting because of its ability to participate in novel chemistry, such as those involved in the depletion of the ozone layer.[1] Surface reactions are totally different from the analogous process in the homogeneous bulk phase, and those of ice are no exception.[2] This makes reactions at ice surfaces interesting. Alcohol molecules present in the atmosphere play a vital role in the chemistry of the troposphere; especially in the ozone cycle in the upper troposphere.[3] *n*-Butanol (NBA) is notable among the alcohols that are present in the upper atmosphere, and the need for investigating the ice−butanol system is due to its environmental relevance. NBA goes into the atmosphere through various channels; some of them include evaporation from solvents, sewage treatment, manufacturing of starch and whiskey, wood pulping, and turbine emissions. Relatively high concentration of NBA was found at Point Barrow, Alaska, when compared to other possible simple hydrocarbons.[4] There are a few publications on both experimental and computational studies of simple alcohols, methanol,[5] ethanol,[3,6] and propanol,[11] on ice surfaces. Theoretical studies exist on NBA and TBA, both in the liquid and in the solid phases.[7] Nishikawa et al.[8] studied the structure of TBA and water mixtures by X-ray diffraction. Souda et al. have done substantial work on methanol,[9] ethanol,[10] and propanol[11] interaction with ice films by using time of flight-secondary ion mass spectrometry (TOF-SIMS). To the best of our knowledge, there is no literature on an NBA−amorphous solid water (ASW) system. Hence, the present study was performed in order to fill the gap in our understanding of the interaction of solid butanol and ice which may have some relevance to the atmosphere. The present study is a continuation of our previous work on ice films using the highly surface sensitive low energy ion scattering technique.[12−14] In the first two, we examined atmospherically relevant molecules on ice surfaces.

The physical properties of a liquid depend on many factors, which include chain length and structure of the molecule. NBA is partially miscible with water, and its solubility is approximately 8 g per 100 g of water,[15] whereas the first three primary alcohols are completely miscible with water at all proportions. The solubility of butanol increases as the chain branches increase; hence, TBA is completely soluble in water, whereas NBA is only partially soluble. When looked into the molecular level details of water−alcohol interaction, many interesting results were obtained. In one such study, Bako et al.[16] reported the concentration dependent structural changes of water with methanol. Water forms short chain-like structures at higher methanol concentrations, but a percolated network structure is formed at lower methanol concentrations. According to them, the chain-like structure of methanol molecules changes into a ring-like structure upon adding water of a particular concentration. Addition of small amounts of water enhances the packing and self-assembly of alcohol. Although solvation of alcohol was known for a long time, the solvation of methanol[17] and TBA[18] in water looks different at a molecular level. Freezing temperature of water increases upon increasing the number of carbon atoms in the backbone of alcohol.[20] It was also found that shorter chain lengths were associated with increased molecular motion in the alcohol film, which resulted in the decrease of hydrogen bond strength between alcohol's OH group and the interfacial water molecules.[19] Most of the studies done on butanol and water mixtures are in the liquid phase, and their solid state behavior was not really explored. Here, we made an attempt to explain the interaction of these

* To whom correspondence should be addressed. Fax: 91-44-2257-0545 /0509. E-mail: pradeep@iitm.ac.in.
† Current address: Department of Chemistry, Purdue University, West Lafayette, Indiana 47907.

10.1021/jp902020e CCC: $40.75
Published on Web 07/15/2009

atmospherically relevant molecules in the solid phase to probe their molecular behavior at low temperatures and in UHV conditions. The results were compared with the analogous methanol/ethanol/propanol−water ice systems.

There are many experimental techniques available to study the interaction of atmospherically relevant molecules with ice particles. Some of them include, temperature programmed desorption mass spectrometry (TPD MS),[20−23] reflection absorption infrared spectroscopy (RAIRS),[24−26] secondary ion mass spectrometry (SIMS), and temperature-programmed time-of-flight SIMS (TP-TOF-SIMS).[11,27] All of these techniques have advantages as well as disadvantages, and each one was used in order to get specific information about the nature of interaction and the molecular details of the species of interest. Another promising technique named low-energy ion scattering and the associated phenomenon called chemical sputtering[28] are also used to study ice surfaces. This is also known as low energy sputtering (LES), which has been used for surface studies.[29,30] It is a hyper-thermal energy process in which charge exchange between the projectile ion and the surface occurs upon collision of ions in the energy range of 10−100 eV, and the very top surface species are released as ions or neutrals.[28,31,32] This is different from normal sputtering during SIMS, where the ionized particles are emitted when a solid/liquid surface is bombarded by particles, typically having keV energies. The energy of the primary beam in SIMS is transferred to the atoms/molecules on the surface by a cascade of collisions. It is important to note that the surface sensitivity in low energy ion scattering experiments can be as high as the first few monolayers (MLs) for an ice film. We have used the chemical sputtering technique for all of our studies as low energy ions are potential candidates for probing the surface properties of ice and other molecular solids. Our present study gives a basic understanding of the diffusive miscibility of NBA and TBA. The findings from this study were compared with the previous studies of interaction of carboxylic acids with ice surfaces.[12]

2. Experimental Section

The instrumental setup and an outline of the experiment are given elsewhere.[12−14] Briefly, the experiments described here were conducted in a double-chamber ultrahigh vacuum (UHV) system with a base pressure of $<5.0 \times 10^{-10}$ mbar. Each region of the system is pumped by a Pfeiffer (TMU 261) 210 L/s turbo molecular drag pump. These two pumps are backed by another Pfeiffer (TMU 071P) 60 L/s turbo molecular pump which is further backed by a Pfeiffer (MVP 055) 3.3 m^3/h dry pump. In the present experiment, mass selected Ar^+ (m/z 40) ions produced by 70 eV electron impact (EI) of Ar, in a source block maintained at varying potential, are mass selected and collided at the ice surface at specific collision energy. By varying the potential of the ion source block and tuning the rest of the ion optics, it was possible to produce a beam current of 1−2 nA. The Ar^+ ions collide with the surface at an angle of 45° with reference to the surface normal, and the scattered ions were analyzed by a quadrupole mass analyzer (Q3). A high-precision UHV specimen translator with xyz axis movement and tilt was used. Polycrystalline copper was used earlier as the substrate material for preparing amorphous and crystalline ice films.[33] We have used the same as the substrate in the present as well as in our earlier studies.[12−14] Substrate plays a crucial role in determining the quality of the grown film, but in the present case, the effect of substrate is negligible because of the higher coverages used. Crystallization induced dewetting,[34] and consequent exposure of the underlying copper surface is very unlikely at such a large thickness. It has been noted that the dewetting temperature is much higher (∼160 K) for 50 ML ice films.[35] The ice film grown in ultrahigh vacuum is known to be amorphous in nature (or amorphous solid water, ASW), while deposition above 140 K results in crystalline ice (CW).[36,37] The ice surface is prepared by exposing water vapor at specific pressure as described below. The scattered ions are collected and mass analyzed. The liquids used in our study, namely, H_2O, D_2O, NBA, and TBA, were purified by many freeze−pump−thaw cycles, before use. NBA was purchased from Rankem chemicals, and TBA was purchased from Spectra chemicals. D_2O was purchased from Aldrich chemicals, and deionized water after triple distillation was used for preparing solid water. Molecular surfaces were prepared by depositing the corresponding vapors, which were exposed to the sample plate through a leak valve. The gas-line was pumped thoroughly by a rotary pump to avoid impurities and contamination. The distance between the sample source tube and polycrystalline copper substrate was adjusted to obtain uniform sample growth on the substrate. Delivery of molecules near the substrate ensures that the vapors are not deposited in unwanted areas. The deposition flux of the vapors was adjusted to ∼0.1 ML/s. The thickness of the overlayers was estimated assuming that 1.33×10^{-6} mbar/s = 1 ML. In all our experiments, the deposition temperature was kept at 110 K. The partial pressure(s) of the gas(es) inside the scattering chamber during deposition time was 1×10^{-7} mbar. After deposition of a given molecule A, a 5 min time delay was allowed before the deposition of the next molecule B, to prepare A@B (the symbolism implies the creation of layer B over A). This was to ensure that B was free from any contamination by A. Several systems were prepared to study diffusive miscibility of NBA. For example, 100 MLs of NBA was deposited first on Cu substrate followed by 100 MLs of ASW, resulting in NBA@ASW, which was used for the study of NBA diffusion through ice overlayers. The other systems for the study were also prepared in the same manner. The temperature dependence on the structural changes was studied by raising the temperature at 5 K/min and monitoring the sputtering spectrum as a function of temperature. Ar^+ of 30 eV collision energy was used as projectile ion in all our experiments. The spectra presented here were averaged for 100 scans, and the data acquisition time was approximately 0.5 s per scan. The present instrumental setup does not allow TPD measurements.

3. Results and Discussion

3.1. Chemical Sputtering of NBA via Low Energy Ar^+. To understand the dissociative ionization of NBA and its fragmentation pattern induced by low energy Ar^+, 100 MLs of NBA over polycrystalline copper surface (Cu@100 ML NBA) was made. Chemical sputtering from the NBA surface starts >25 eV collision energy of Ar^+, and it shows that NBA can be detected by the low energy ion scattering technique. The mass spectrum, due to 30 eV Ar^+ collision, presented in Figure 1a shows the characteristic features of NBA, but the molecular ion peak (m/z 74) was absent in all our spectra. In the EI mass spectra of NBA, the molecular ion peak is only ∼1.5% of the base peak intensity, and it is absent in the case of TBA.[38] This explains the absence of molecular ion peak in our experiments. Certain other peaks were also absent, which might be due to the differences in the nature of ionization in low energy ion impact. Assignment of the fragmented species was done with reference to the report by Zavilopulo et al.[39] on the dissociative ionization of ethanol, methanol, and butanol. The peak at m/z 15 is due to CH_3^+, and the peak at m/z 27 is due to $C_2H_3^+$. The peaks at m/z 29 and m/z 31 are due to $C_2H_5^+$ and CH_3O^+. Our

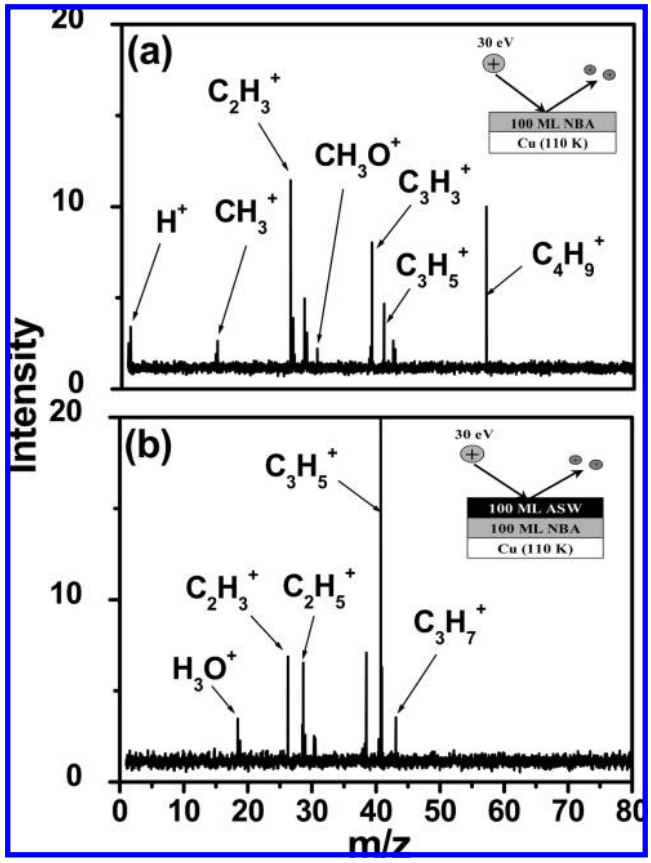

Figure 1. Mass spectra corresponding to 30 eV collisions of Ar^+ at (a) 100 ML NBA and (b) 100 ML NBA@100 ML ASW. Idealized schematic representations of the samples prepared are shown as insets.

peak assignment differs slightly from that of Zavilopulo et al., where they have assigned *m/z* 41 and 43 to C_2HO^+ and $C_2H_3O^+$, respectively. We believe that the peaks at *m/z* 41 and 43 are due to $C_3H_5^+$ and $C_3H_7^+$ and not due to C_2HO^+ and $C_2H_3O^+$, respectively. Other than this difference, all the other remaining peak assignments are the same. The peak at *m/z* 39 may be due to $C_3H_3^+$. The base peak at *m/z* 56 in the EI spectrum is absent in the chemical sputtering spectrum. Instead, a peak at *m/z* 57 is seen, which is assigned to $C_4H_9^+$. The absence of the peak is related to the nature of fragmentation, dissociation, and ion ejection upon low energy ion impact.

3.2. Diffusivity of NBA through ASW. Molecular intermixing of NBA with ice was one of our interests which urged us to do the present study. To understand the diffusivity of NBA through water−ice, ASW was deposited over NBA (100 ML NBA@100 ML ASW). The corresponding mass spectrum is shown in Figure 1b. The inset of the figure gives a schematic representation of the sample and shows the situation where no interlayer diffusion occurs. The sharp boundary between the phases presents only an idealized view. The substrate temperature was constant at 110 K. From the chemically sputtered species, the presence of NBA molecules, which appeared over the ASW layer by diffusion, was confirmed. H_2O was present on the top surface, as seen in the mass spectrum. The peak at *m/z* 19 is due to H_3O^+, which is formed as a result of proton transfer reaction as a result of Ar^+ collsions.[40]

$$2H_2O \rightarrow H_3O^+ + OH^-$$

This reaction explains the formation of protonated molecular ions in the scattering spectrum of pure H_2O and D_2O surfaces, which are shown in Figure S1 (Supporting Information). As in the case of NBA, and that reported previously,[12] chemical sputtering species from the ASW surface were observed 25 eV onward. CH_3^+ is absent when ASW was deposited over NBA (Figure 1b). The spectrum (Figure 1b) clearly has the features of both H_2O and NBA; however, some of the features seen in the spectrum of pure NBA are absent. Most significantly, $C_4H_9^+$ and CH_3^+ are absent, and several others have varying intensity. We attribute these differences to the difference in the self-assembled structure of NBA layers on water ice. The presence of the features of H_2O and NBA suggests that both the species are present on the surface. For it to be present at the H_2O surface, NBA has to diffuse through the water over layers. Presumably, the structure of NBA present within the ice matrix does not allow the $C_4H_9^+$ species to be formed. This can be attributed to the formation of multiple hydrogen bonding interactions with several water molecules and subsequent strengthening of the C−O bond in alcohol, which inhibits the formation of $C_4H_9^+$. On the contrary, the species such as $C_3H_5^+$ and $C_3H_7^+$ are formed. This suggests that NBA is unlikely to have a preferred orientation at the surface with alkyl chains projecting upward with the OH group anchoring on the surface. Such a geometry would have allowed ion neutralization at the hydrocarbon chain ends, allowing the formation of CH_3^+ and $C_4H_9^+$. Thus, the structure of the NBA surface is inferred to be disordered. It may be noted that the surface structure of the desorbing species determines the type of ions desorbed upon low energy ion impact.

3.3. Thickness Dependent Studies of NBA with ASW. The diffusive nature of NBA through the hydrogen bonded network of ASW may be inferred from the previous section. However, this needs to be investigated. For this, NBA was deposited on top of ASW (ASW@NBA) at various coverages. The chemical sputtering spectra of this system are shown in Figure 2. When 100 ML NBA was deposited on 100 ML ASW, H_2O was not seen on the surface (see Figure 2a). Diffusion of H_2O through NBA could have taken long for it to reach the surface, and this might be a possible reason for the absence of H_2O. The other reason might be due to the change in the network structure of ASW at the interface such that the water molecules present there are not free to move to the top surface. Self-assembly of the hydrocarbon chains of NBA could be another reason, which prevents the diffusion of H_2O through it. One may also view this as due to the lower surface energy of NBA, which makes it float on the ASW surface, just as in the case of liquid alcohols. Scan time was increased, and repeated scans were made for nearly 30 min; still, H_2O was not visible in the mass spectrum. Hence, the latter three appear to be the important reasons. It is important to note that peaks due to CH_3^+ and $C_4H_9^+$ are present in the spectrum, which suggests that the structure of NBA is similar to that in its pure state. Figure 2b shows the result of a similar kind of experiment, but the thickness of NBA was reduced down to 1 ML in order to see the effect of water diffusion at such low coverages of NBA (100 ML ASW@1 ML NBA). At this condition, NBA is likely to form island-like structures.[35,43] Hence, H_2O was exposed to Ar^+, forming H_3O^+. Some of the specific fragments of NBA such as CH_3^+, $C_3H_7^+$, and $C_4H_9^+$ were absent. This is attributed to the disordered assembly of NBA as in the same situation in Figure 1b. Upon increasing the thickness of NBA, it alone was observed on the surface, and this takes place somewhere between 3−5 MLs, and more than this thickness, diffusive mixing of ASW was stopped completely. There is no difference in the mass spectrum upon increasing the thickness of NBA coverage. Figures 2c and

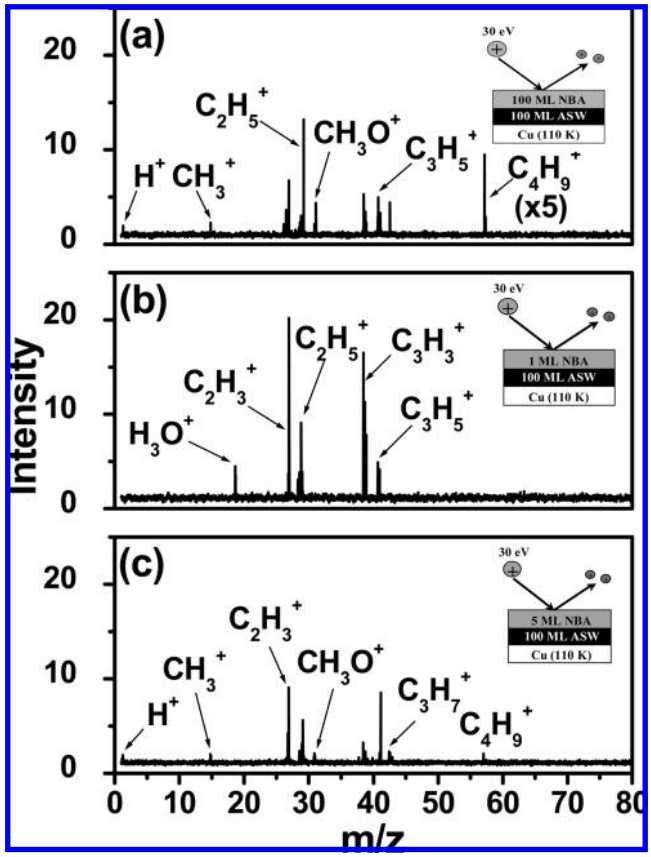

Figure 2. Chemical sputtering spectra of (a) 100 ML ASW@100 ML NBA, (b) 100 ML ASW@1 ML NBA, and (c) 100 ML ASW@5 ML NBA.

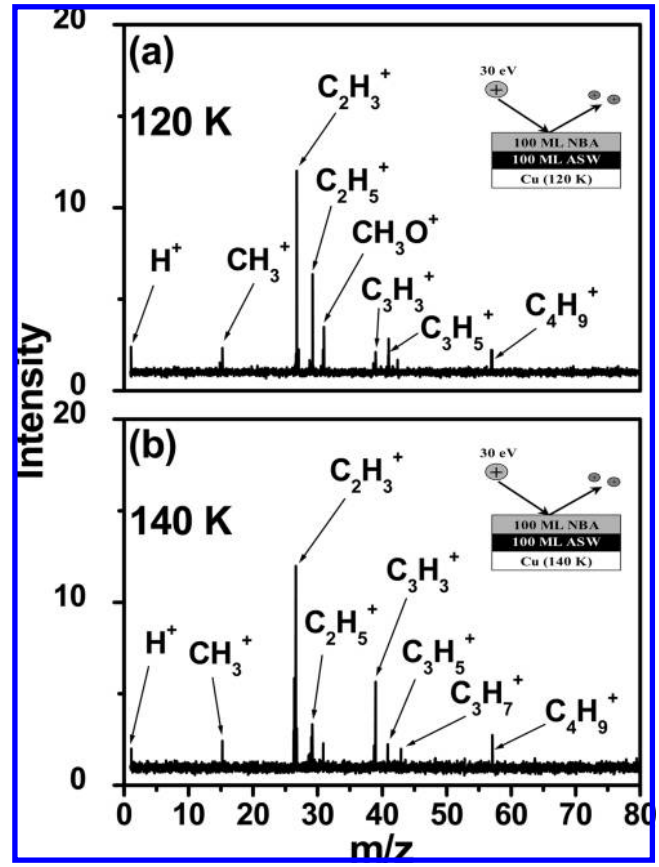

Figure 3. Chemical sputtering spectra of 100 ML ASW@100 ML NBA at different substrate temperatures, (a) 120 K and (b) 140 K.

a look similar, except for the change in intensity which indicates that ASW could not penetrate through more than 3−5 MLs thick NBA, or it always floats on ASW layers as expected in the liquid state. When NBA diffuses through H_2O, the structure of the former is different. Comparing Figures 1b and 2a, it is clear that NBA is present on both the surfaces, while H_2O is absent in the second case. It is also clear that the way in which NBA presents itself on the two surfaces is different. While the CH_3^+ and $C_4H_9^+$ features are absent when NBA diffuses through H_2O, they are present when NBA is deposited on ice. These are also present when it is deposited directly on Cu. These aspects clearly suggest that the structure of NBA layers deposited on H_2O and Cu is the same, while that of diffused NBA is different.

3.4. Solvation of ASW and Hydration of NBA. To understand the effective thickness at which the diffusive mixing of NBA is blocked through ASW, increasing ASW layers were made over NBA. The thickness of ASW was gradually increased from 100 to 1000 MLs, and NBA molecules were seen even at the highest coverage (100 ML NBA@1000 ML ASW). The spectrum shown in Figure S2a (Supporting Information) corresponds to 100 ML NBA@1000 ML ASW. It is clear that NBA is present on top surface layers. There can be two pathways through which NBA could possibly diffuse through ASW. One may be through micropores of ASW and the other one through the network structure of ASW. Our study does not distinguish the two paths. Assuming a change in orientation of NBA during the process of diffusive mixing, as revealed by the data, these molecules are exposed to Ar^+ in certain preferred orientations. It appears that the alkyl chain of NBA is not standing upright, which makes the preferential ejection of CH_3^+ impossible. Hence, only selected fragmented ions are formed from NBA due to ion collision at higher thickness of ASW over NBA. The H^+ and several hydrogen containing carbon fragments are absent in the chemical sputtering spectra. The mass spectrum shown in Figure S2a (Supporting Information) looks similar to that of Figure 2b except for some minor change in the intensity of the peaks. The energy needed for NBA diffusion might be lower than that of H_2O, and hence, the former moves to the surface, whereas H_2O gets retained at the bottom.

3.5. Effect of Temperature on NBA−ASW Interaction. In order to understand the effect of temperature on NBA−ASW interaction, the substrate temperature was increased gradually from 110 to 150 K at a heating rate of 5 K/min with simultaneous monitoring of the sputtered species at 30 eV collision energy. The spectra collected at two different temperatures, 120 and 140 K, are shown in Figure 3. It was thought that annealing at 120 K may help in partially breaking the solvation sphere. Considering the crystallization temperature of ASW to be ∼140 K,[41] we raised the temperature to this value and waited to see some changes in the mass spectrum. We expected H_2O to migrate to the surface through NBA, but in contrast to our expectation, there was no change in the overall spectrum, and H_2O features were still absent as in the case of ASW@NBA at 110 K (see Figure 2a). There are some changes in the intensity of NBA features at 140 K which might be due to the structural difference of solid H_2O and enhancement in the mobility of H_2O at 140 K.[42,43] During the course of our experiments, we found the desorption temperature of NBA to be around 140−145 K, as seen by the pressure gauge. This temperature is likely to have an error of ± 3K. At this temperature range, there was a sudden increase in pressure, indicating that NBA molecules are desorbing from the surface. The desorption temperature of H_2O is well above that of NBA,

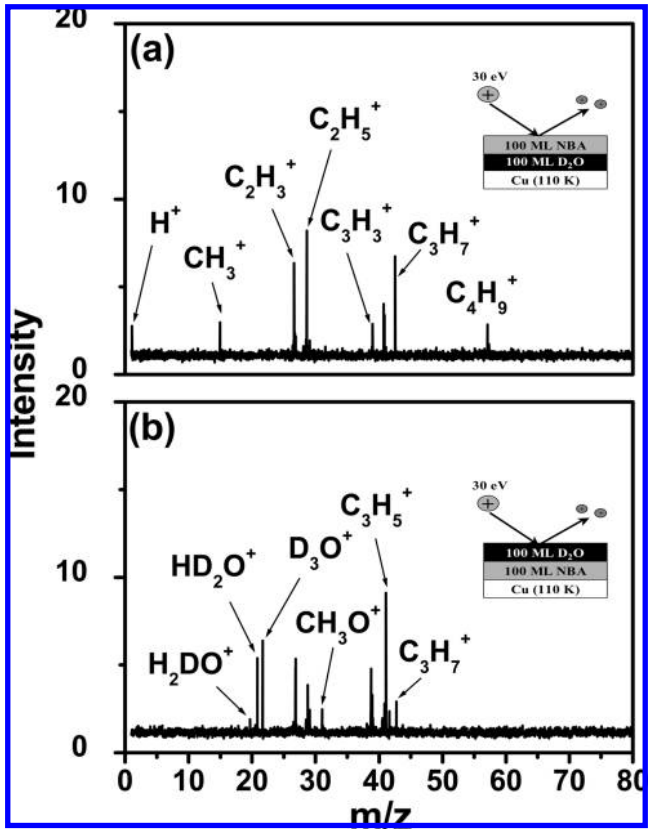

Figure 4. Chemical sputtering spectra of (a) 100 ML D_2O@100 ML NBA and (b) 100 ML NBA@100 ML D_2O.

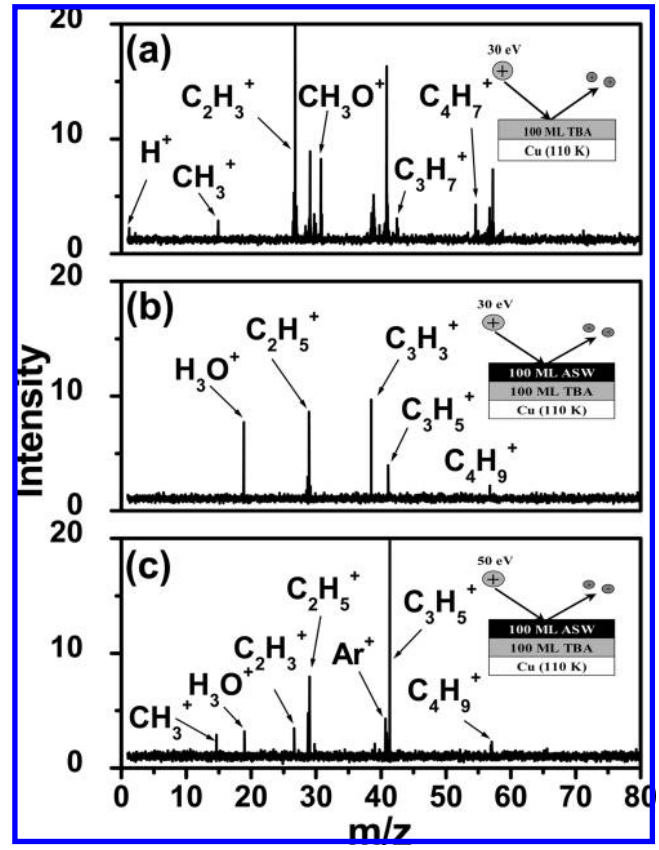

Figure 5. (a) Chemical sputtering mass spectrum of 100 ML TBA at 30 eV collisions of Ar^+. Mass spectra corresponding to (b) 30 eV and (c) 50 eV collisions of Ar^+, respectively, at 100 ML TBA@100 ML ASW.

but at temperatures greater than the desorption temperature of NBA, H_2O was not seen. The reason for this might be due to codesorption of H_2O with NBA. Such codesoprtion is reported in the case of alcohols of lower chain length.[43]

3.6. Proton Transfer between NBA and D_2O. Our next objective was to find if any proton transfer occurs between ASW and NBA due to LES. To address this problem, D_2O was used to make ASW, and 100 ML D_2O@100 ML NBA was made. The data are shown in Figure 4. From the figure, it is evident that there is no effect of D_2O on NBA in terms of proton transfer; hence, there is no change in the mass spectrum of the hydrocarbon fragments, and it looks similar to the one shown in Figures 1a and 2a, except for the difference in H_2O and D_2O features. Both the molecular solids, namely, H_2O and D_2O, behave similarly with NBA at 110 K. H/D exchange between NBA and D_2O is likely as NBA diffuses through ASW. This could be the reason for the increased intensity of the exchanged peaks (H_2DO^+ and HD_2O^+) in comparison to the spectrum presented in Figure S1a (Supporting Information).

3.7. Diffusion, Proton Transfer, and Temperature Dependent Studies of the TBA−ASW System. We have extended the studies to an isomer of butanol, namely, TBA, which has a branched structure. As mentioned earlier, TBA is completely soluble in water, but its miscibility behavior at the molecular level in the solid state is in fact a valuable study to answer some of the fundamental questions of TBA−ASW interaction. We have repeated all of the experiments performed on the NBA−ASW system on this system as well. Figure 5a shows the chemical sputtering spectrum of TBA at 30 eV Ar^+, and Figure 5b shows its diffusive behavior through ASW at 110 K. In order to see the effect of collision energy on the chemically sputtered species, we have increased the collision energy to 50 eV and monitored the mass spectrum. More fragmentation was observed with increasing collision energy (Figure 5c). The effect of thickness of TBA on ASW is shown in Figure S3 (Supporting Information). It is clear that TBA behaves in a fashion similar to that of NBA in terms of diffusive mixing. Increase in thickness of ASW even to 1000 MLs does not block TBA diffusive mixing through ice, and this is shown in Figure S2b (Supporting Information). The effect of temperature on the TBA−ASW system was also studied, and this is shown in Figure S4 (Supporting Information). No qualitative changes were seen in TBA, in comparison to those in NBA. We conclude that both NBA and TBA behave similarly with H_2O and D_2O in the solid state. It is clear that structure of the chain may not be the only reason for inhibiting the diffusion of water through alcohol overlayers.

We have also done experiments with methanol (CH_3OH@ASW) and ethanol (C_2H_5OH@ASW) (data in Figure S5, Supporting Information), which clearly show that water could diffuse through both the alcohols. However, water could not diffuse through propanol (C_3H_7OH@ASW) (see Figure S6, Supporting Information) because of longer chain length, as in the case of NBA. The hydrophilic nature and size effect could be the possible reasons for the observed behavior of methanol and ethanol. Complexity of the network structure of alcohol molecules increases as the chain length increases. Self-assembly of lower chain alcohols might not be continuous over larger areas and in-turn allows ASW to diffuse through, whereas long chain alcohols might have greater tendency for self-assembly with greater packing efficiency. NBA has been investigated more thoroughly here because of its atmospheric relevance. We find that both the molecular solids, namely, H_2O and D_2O, behave

in a similar manner in terms of their diffusivity and mixing with the alcohol molecules.

4. Summary and Conclusions

The ion scattering experiment described here finds the incomplete diffusive mixing of two alcohol molecules, namely, NBA and TBA, with water ice in the temperature range of 110−150 K. In all our experiments, we have used Ar^+ as the projectile ion in the 30−50 eV collision energy range. It is clear that NBA diffuses through ASW layers and that both species occur on the surface when ASW is deposited on NBA. On the contrary, water is not seen when NBA is deposited over ASW. This could be attributed to the absence of diffusive mixing or surface segregation of alcohols as in the liquid state. Both D_2O and TBA behave in a manner similar to that of their isomeric analogues. Although the presence of NBA and TBA is detected, while ASW is present, both the alcohols undergo selective ionization, which gives specific peaks in the mass spectrum. The mechanism for this is not known exactly. The diffusive miscibility of NBA in H_2O was observed even up to 1000 MLs of ASW. The results suggest that long chain alcohols may act as barriers for H_2O diffusion because of their hydrophobic nature. Increase in the chain length inhibits the motion of H_2O. Self-assembly of longer chain alcohols creating denser overlayers could be the prime reason for the incomplete diffusion of ASW. While lower chain alcohols, methanol and ethanol, show complete diffusion or no surface segregation, incomplete diffusion or surface segregation starts with propanol. The results may have relevance to the fate of NBA and TBA in the atmosphere of Earth.

Acknowledgment. We thank the DST, Government of India, for supporting our research program. G.N.K. thanks D. M. David Jeba Singh for his critical suggestions in preparing the manuscript. The instrument was built using the support of a Swarnajayanti Fellowship awarded to T.P.

Supporting Information Available: Chemical sputtering spectra of (1) pure H_2O and D_2O, (2) diffusive mixing of TBA and NBA through H_2O overlayers, (3) diffusive mixing of H_2O through TBA overlayers, (4) spectra of TBA and H_2O at different substrate temperatures, (5) diffusive mixing of H_2O through methanol and ethanol, and (6) diffusive mixing of H_2O through propanol. This material is available free of charge via the Internet at http://pubs.acs.org.

References and Notes

(1) Molina, M. J.; Tso, T.-L.; Molina, L. T.; Wang, F. C.-Y. *Science* **1987**, *238*, 1253.
(2) Kang, H. *Acc. Chem. Res.* **2005**, *38*, 893.
(3) Peybernès, N.; Calvé, S. L.; Mirabel, P.; Picaud, S.; Hoang, P. N. M. *J. Phys. Chem. B* **2004**, *108*, 17425.
(4) Cavanagh, L. A.; Schadt, C. F.; Robinson, E. *Environ. Sci. Technol.* **1969**, *3*, 251.
(5) Wu, C. Y. R.; Yang, B. W.; Judge, D. L. *Planet. Space Sci.* **1994**, *42*, 273.
(6) Thierfelder, C.; Schmidt, W. G. *Phys. Rev. B* **2007**, *76*, 195426.
(7) Sokolov, O.; Abbatt, J. P. D. *J. Phys. Chem. A* **2002**, *106*, 775.
(8) Nishikawa, K.; Iijima, T. *J. Phys. Chem.* **1990**, *94*, 6227.
(9) Souda, R. *Phys. Rev. B* **2007**, *75*, 184116.
(10) Souda, R. *J. Chem. Phys.* **2005**, *122*, 134711.
(11) Souda, R. *Phys. Rev. B* **2004**, *70*, 165412.
(12) Cyriac, J.; Pradeep, T. *J. Phys. Chem. C* **2007**, *111*, 8557.
(13) Cyriac, J.; Pradeep, T. *J. Phys. Chem. C* **2008**, *112*, 1604.
(14) Cyriac, J.; Pradeep, T. *J. Phys. Chem. C* **2007**, *111*, 5129.
(15) *International Critical Tables of Numerical Data, Physics, Chemistry, and Technology*; Washburn, E. W., Ed.; McGraw-Hill: New York, 1928; Vol. III.
(16) Bakó, I.; Megyes, T.; Bálint, S.; Grósz, T.; Chihaia, V. *Phys. Chem. Chem. Phys.* **2008**, *10*, 5004.
(17) Dixit, S.; Soper, A. K.; Finney, J. L.; Crain, J. *Europhys. Lett.* **2002**, *59*, 377.
(18) Bowron, D. T.; Soper, A. K.; Finney, J. L. *J. Chem. Phys.* **2001**, *114*, 6203.
(19) Popovitz-Biro, R.; Wang, J. L.; Majewski, J.; Shavit, E.; Leiserowitz, L.; Lahav, M. *J. Am. Chem. Soc.* **1994**, *116*, 1179.
(20) Park, S. C.; Kang, H. *J. Phys. Chem. B* **2005**, *109*, 5124.
(21) Smith, R. C.; Huang, C.; Wong, E. K. L.; Kay, B. D. *Phys. Rev. Lett.* **1997**, *79*, 909.
(22) Sadtchenko, V.; Knutsen, K.; Giese, F. C.; Gentry, W. R. *J. Phys. Chem. B* **2000**, *104*, 2511.
(23) McClure, S. M.; Barlow, E. T.; Akin, M. C.; Safarik, D. J.; Truskett, T. M.; Mullins, C. B. *J. Phys. Chem. B* **2006**, *110*, 17987.
(24) Maté, B.; Medialdea, A.; Moreno, M. A.; Escribano, R.; Herrero, V. J. *J. Phys. Chem. B* **2003**, *107*, 11098.
(25) Faradzhev, N. S.; Perry, C. C.; Kusmierek, D. O.; Fairbrother, D. H.; Madey, T. E. *J. Chem. Phys.* **2004**, *121*, 8547.
(26) Gane, M. P.; Williams, N. A.; Sodeau, J. R. *J. Phys. Chem. A* **2001**, *105*, 4002.
(27) Kondo, M.; Kawanowa, H.; Gotoh, Y.; Souda, R. *Surf. Sci.* **2005**, *594*, 141.
(28) Cooks, R. G.; Ast, T.; Mabud, A. Md. *Int. J. Mass Spectrom. Ion Processes* **1990**, *100*, 209.
(29) Pradeep, T.; Shen, J.; Evans, C.; Cooks, R. G. *Anal. Chem.* **1999**, *71*, 3311.
(30) Cooks, R. G.; Ast, T.; Pradeep, T.; Wysocki, V. H. *Acc. Chem. Res.* **1994**, *27*, 316.
(31) Grill, V.; Shen, J.; Evans, C.; Cooks, R. G. *Rev. Sci. Instrum.* **2001**, *72*, 3149.
(32) Vincenti, M.; Cooks, R. G. *Org. Mass Spectrom.* **1988**, *23*, 317.
(33) Trakhtenberg, S.; Naaman, R.; Cohen, S. R.; Benjamin, I. *J. Phys. Chem. B* **1997**, *101*, 5172.
(34) Stähler, J.; Mehlhorn, M.; Bovensiepen, U.; Meyer, M.; Kusmierek, D. O.; Morgenstern, K.; Wolf, M. *Phys. Rev. Lett.* **2007**, *98*, 206105.
(35) Kimmel, G. A.; Petrik, N. G.; Dohnálek, Z.; Kay, B. D. *J. Chem. Phys.* **2007**, *126*, 114702.
(36) Stevenson, K. P.; Kimmel, G. A.; Dohnálek, Z.; Smith, R. S.; Kay, B. D. *Science* **1999**, *283*, 1505.
(37) Zondlo, M. A.; Onasch, T. B.; Warshawsky, M. S.; Tolbert, M. A.; Mallick, G.; Arentz, P.; Robinson, M. S. *J. Phys. Chem. B* **1997**, *101*, 10887.
(38) Mallard, G.; Linstrom, P. J. NIST Standard Reference Data Base, *69*, 2000.
(39) Zavilopulo, A. N.; Chipev, F. F.; Kokhtych, L. M. *Nucl. Instrum. Methods Phys. Res., Sect. B* **2005**, *233*, 302.
(40) Souda, R. *J. Phys. Chem. B* **2004**, *108*, 283.
(41) Minoguchi, A.; Richert, R.; Angell, C. A. *Phys. Rev. Lett.* **2004**, *93*, 215703.
(42) Souda, R.; Kawanowa, H.; Kondo, M.; Gotoh, Y. *J. Chem. Phys.* **2003**, *119*, 6194.
(43) Souda, R. *J. Chem. Phys.* **2003**, *119*, 2774.

JP902020E